

Numerical Simulation of Torrential Rainfall and Vortical Hot Towers in a Midlatitude Mesoscale Convective System

ZHANG Man^{1,2,3}, Da-Lin ZHANG³, and WANG Ang-Sheng¹

¹*Institute of Atmospheric Physics, Chinese Academy of Sciences, Beijing 100029, China*

²*Graduate University of the Chinese Academy of Sciences, Beijing 100049, China*

³*Department of Atmospheric and Oceanic Science, University of Maryland, College Park, Maryland 20742, USA*

Received 19 April 2009; revised 14 June 2009; accepted 14 June 2009; published 16 July 2009

Abstract A cloud-resolving model simulation of a mesoscale convective system (MCS) producing torrential rainfall is performed with the finest horizontal resolution of 444 m. It is shown that the model reproduces the observed MCS, including its rainfall distribution and amounts, as well as the timing and location of leading rainbands and trailing stratiform clouds. Results show that discrete convective hot towers, shown in Vis5D at a scale of 2–5 km, are triggered by evaporatively driven cold outflows converging with the high- θ_e air ahead. Then, they move rearward, with respect to the leading rainbands, to form stratiform clouds. These convective towers generate vortical tubes of opposite signs, with more intense cyclonic vorticity occurring in the leading convergence zone. The results appear to have important implications for the improvement of summertime quantitative precipitation forecasts and the understanding of vortical hot towers, as well as midlevel mesoscale convective vortices.

Keywords: torrential rainfall, mei-yu front, vortical hot towers, mesoscale convective systems

Citation: Zhang, M., D.-L. Zhang, and A.-S. Wang, 2009: Numerical simulation of torrential rainfall and vortical hot towers in a midlatitude mesoscale convective system, *Atmos. Oceanic Sci. Lett.*, **2**, 189–193.

1 Introduction

It is well-known that mesoscale convective systems (MCSs) are responsible for a large portion of daily precipitation around the globe (Houze, 2004). This is especially true in East Asia, where MCSs that develop along mei-yu fronts, which are characterized by large horizontal moisture gradients, account for most of the rainfall totals during the growing season (Chen et al., 1998). Because of their quasi-stationary nature, flood disasters often occur over the Yangtze and Huai river basins when a series of intense convective cells propagate over the same area along a mei-yu front.

Despite considerable research in the past decades, the ability to predict and understand torrential rainfall along the mei-yu front is very limited due to the lack of high-resolution observations. Heavy rainfall, after all, is an end product of multi-scale nonlinear interactions ranging from cloud microphysical processes to cloud dynamics, as well as MCSs and mei-yu frontal circulations. Although several field observations have been conducted in East Asia

during the past few decades (e.g., the Taiwan Area Mesoscale Experiment in 1987 and the Huai-River Basin Experiment in 1998), they have only provided snapshots of MCSs and the mei-yu frontal systems. The limited spatial and temporal resolutions in today's observations make cloud-resolving models a viable option for studying the multi-scale interactions involved in the development of MCSs and the mei-yu fronts, as well as their associated rainfall.

Previous real-data modeling studies of mei-yu frontal precipitation have been restricted by coarse resolution, imperfect initial conditions, and crude physical parameterizations. Up until now, the finest model grid size used for mei-yu front studies has been about 2 km (Kato, 2006). This type of grid size can only resolve large, organized cumulonimbi (i.e., with a scale greater than 12 km). However, many meso- γ -scale circulations, such as localized intense rainfall, convective downdrafts and vortices, and linear rainbands, are too small to be adequately resolved. Intense convective overturning, in particular, always tends to occur at the smallest resolvable scale. Thus, it is desirable to use grid resolutions as high as possible in order to more realistically reproduce the convective cloud structures and to evaluate the multi-scale interactions involved in the production of heavy rainfall in MCSs or along mei-yu fronts.

The purposes of this study were to (a) demonstrate the cloud-resolving predictability of heavy rainfall events along a mei-yu front and (b) investigate the three-dimensional (3-D) structures of vortical hot towers (VHTs) (as recently shown by Hendricks et al. (2004) for tropical cyclones) in relation to the organization of MCSs, as well as heavy rainfall, using Vis5D which is an animated 3-D visualization system. This was achieved by using an 12-h cloud-resolving simulation of a mei-yu frontal MCS that produced flooding rainfall in East China with the finest grid resolution of 444 m.

The next section briefly describes the major model features used for the study. Section 3 presents a brief overview of the case, and shows the 3-D structures of VHTs after verifying the simulated precipitation and radar reflectivity against the observed data. A summary and concluding remarks are given in the final section.

2 Model description

A two-way interactive, quadruple-nested grid (12/4/1.33/0.44 km), which is a nonhydrostatic version of the

Penn State University/National Center for Atmospheric Research model (MM5, mesoscale model 5) version 3.6 (Dudhia, 1993), was used to simulate a heavy rainfall case with the finest grid size of 444 m. The (x, y) dimensions of the four nested domains, from the outermost (D01) to the innermost (D04), were 202×232 (D01), 385×391 (D02), 385×391 (D03), and 385×391 (D04), respectively. In the vertical coordinate, 40 (terrain-following) σ -levels were used with higher resolutions in the planetary boundary layer (PBL). The model top was defined at 30 hPa. The model physics used included the Blackadar PBL scheme (Zhang and Anthes, 1982), a cloud-radiation interaction scheme, the Kain-Fritsch cumulus parameterization (Kain, 2004), and the Tao and Simpson (1993) three-ice cloud microphysics scheme. No cumulus parameterization was used for the two finest resolution domains D03 and D04. Otherwise, the above model physics schemes were applied to all four domains.

The model was initialized at 0000 UTC (i.e., 0800 LST) 4 July 2003 using the National Centers for Environmental Prediction's (NCEP) $1^\circ \times 1^\circ$ reanalysis. This was then enhanced by conventional upper-air observations and 5 additional soundings taken upstream from the area of interest during a field campaign. The MCS under study had just begun to form during the early morning hours. The lateral boundary conditions for D01 were specified by the hourly output of a 30-h dynamic-nudging simulation with a grid size of 36 km over a much larger domain. To minimize unnecessary computational costs, D02 was activated six hours into the integration, whereas the cloud-resolving D03 and D04 were activated twelve hours into the integration. A 24-h model integration was conducted ending at 0000 UTC 5 July. This was long enough to cover the life cycle of the MCS, including the generation of the heavy rainfall events of interest.

3 Results

The torrential rainfall events of our interest occurred during the evening hours of 4 July 2003, as a new MCS developed behind a dissipated MCS in the warm air of the mei-yu front over western Anhui Province. Convective cells were seen forming along a line in the wake of the dissipating MCS. The MCS passed through Chuzhou at 0000 UTC 5 July, and it dumped heavy precipitation across Anhui Province, with two localized rainfall centers (Fig. 1a). The 24-h accumulated rainfall amounts, ending 0000 UTC 5 July, were over 100 mm in western Anhui Province and about 274 mm at Chuzhou. Both satellite and radar images (not shown) revealed that most of the heavy precipitation at Chuzhou was generated by the passage of the leading rainband. This rainband consisted of a series of convective cells that successively developed and then propagated northeastward along the mei-yu front. The lesser amount of precipitation that occurred in western Anhui Province appeared to be attributable to the downslope influence of the orography farther west. Fewer intense convective cells developed along the leading rainband after passing Chuzhou, which was likely due to

the decreasing energy supply from the southwesterly flow. Thus, the rainfall amount decreased toward the central Jiangsu Province.

It is encouraging that the model was able to reproduce the general pattern and magnitude of the 24-h accumulated rainfall (Fig. 1a), including the two rainfall centers.

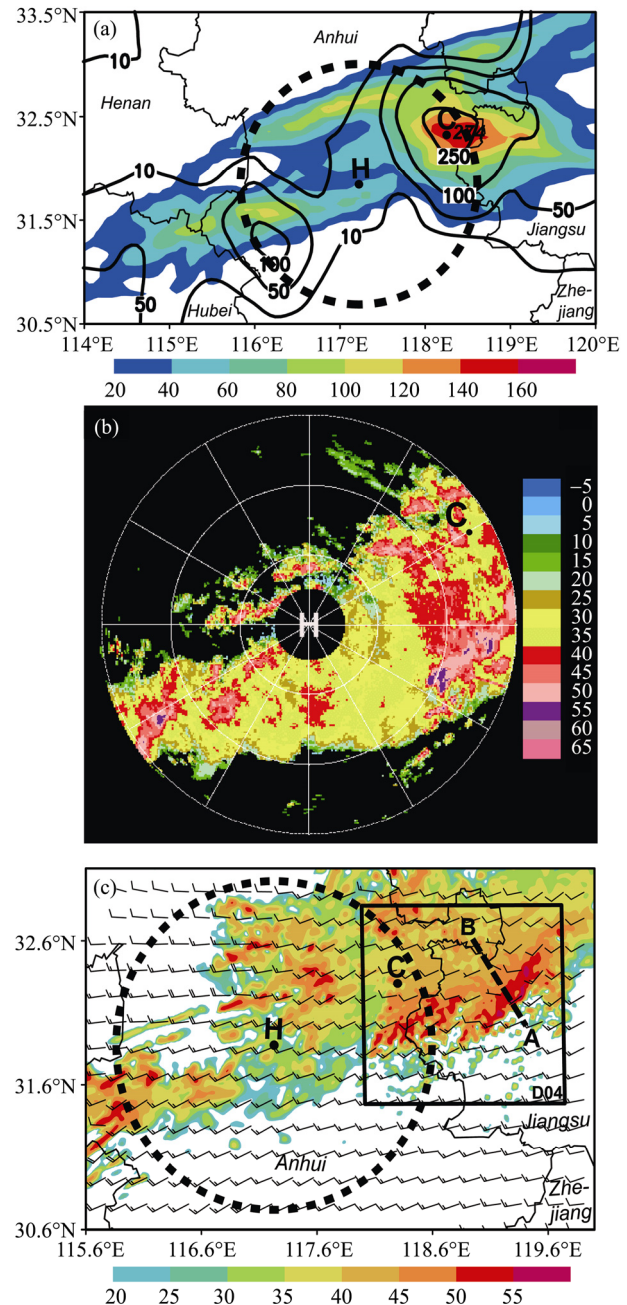


Figure 1 (a) Comparison of the 24-h accumulated rainfall (mm) between the simulated (shadings) and observed (contoured) data ending 0000 UTC 5 July 2003. (b) The observed reflectivity (dBZ) from Hefei's radar at 2000 UTC 4 July 2003. (c) The 20-h (but 8-h for D03 and D04) simulated reflectivity and horizontal winds at 800 hPa; a full barb is 5 m s^{-1} . Letters "C" and "H" denote the station locations of Chuzhou (118.3°E , 32.3°N) and Hefei (117.23°E , 31.87°N), respectively. Dashed lines in (a) and (c) show the maximum radial range (i.e., 150 km) of Hefei's radar. The internal frame in (c) denotes the finest-resolution domain (D04). Line AB denotes the location of a vertical cross section used in Fig. 2.

The rainfall center over western Anhui Province was also reasonably reproduced, though with less coverage to the south. We believe that such an encouraging predictability can be attributed to the more realistic representation of the mei-yu front in the NCEP reanalysis, which was enhanced by a few field observations, as well as the use of more reasonable model physics with a higher grid resolution.

Like the rainfall field, the model-simulated radar reflectivity from both the 1.33-km and 444-m resolution domains, following Liu et al. (1997), compared favorably to that measured at 2000 UTC 4 July (cf. Figs. 1b and 1c), i.e., after the leading rainband had passed Chuzhou. For example, both the observations and the simulations showed the development of an intense rainband to the east of Hefei with a trailing stratiform region. In addition, they showed several scattered but intense echoes to the southwest of Hefei, contributing to the rainfall center over western Anhui Province (cf. Figs. 1a–c). A few intense echoes also occurred near the northwestern edge of the trailing stratiform region, which were likely caused by the overrunning of high- θ_e (equivalent potential temperature) air over the cold downdraft air mass left behind by the leading rainband. These convective cells also appeared to have contributed a significant amount to the total rainfall at Chuzhou as they passed by a few hours later. One can see that our 444-m resolution domain was used to resolve the propagation of convective cells with more intense precipitation over the eastern Anhui Province.

To gain insight into the organization of the MCS, Fig. 2 shows the Vis5D plots of the simulated radar reflectivity, local buoyancy and the vertical component of relative vorticity during the mature stage over the 444-m resolution domain. The local buoyancy was obtained by subtracting a reference virtual temperature field, which was obtained by performing a running average of the model output at 32 neighboring points. Note that non-precipitating cloud water and cloud ice could not be represented in Fig. 2a because they contributed little to radar reflectivity. Apparently, discrete (rather than continuous) convective cells were first initiated in the moist southwesterly monsoon air ahead, followed by robust precipitating towers (as tall as 150 hPa) in the leading (low-level) convergence zone (about 10–15 km wide), and weakening cloud columns with more stratiform precipitating clouds in the rear (Fig. 2a). The melting layer, defined as large vertical gradients in radar reflectivity, was clearly seen (near 550 hPa) across the MCS. The maximum updraft intensity in the leading rainband was as large as 25 m s^{-1} , and it reduced to $1\text{--}2 \text{ m s}^{-1}$ within an hour as it moved rearward. It is interesting that the scales of these deep precipitating towers of varying intensities ranged from 2 to 5 km across the MCS, even in the stratiform region. Given the front-to-rear flow aloft and the rear inflow below (see the area-averaged hodograph in Fig. 2c), this result implies that the precipitating towers in the trailing region could be traced back continuously to their convective origins in the leading rainband, and that they weakened due to a lacking energy supply, having been advected rearward. To our knowledge, such meso- γ -scale 3-D inhomogeneity in the

trailing stratiform region and its relation to the leading deep convective towers have not been discussed in the literature due to the lack of 3-D high-resolution data. This result also differs from that described by Biggerstaff and Houze (1991), in which secondary (mesoscale) rainbands in the stratiform region were related to intense convective clouds in the leading line via the front-to-rear advection of precipitation particles across an intervening transition zone.

Of further interest is the forward tilt of all the precipitating towers in the lowest layers behind the leading convergence zone, with overhanging cloud anvils ahead that are similar to those described in the conceptual model of a hailstorm by Browning et al. (1976). This reveals the generation of moist downdraft outflows by precipitation evaporation that was more intense in the leading precipitating rainbands, as also indicated by the northerly surface winds. The cold outflows, which converged with the southwesterly flow, helped lift the PBL air to the level of free convection, and they promoted the organization of the MCS along the mei-yu front. In contrast, little evidence of such forward tilt appeared for new convective towers ahead (Fig. 2a) because of dominant buoyant upward motion with little precipitation reaching the ground (Fig. 2b).

It is apparent from Fig. 2b that many convective cores in the leading rainband were at least 1°C warmer than their neighboring columns (the so-called “hot towers”), while some buoyant columns reached the upper troposphere. Similarly, negatively buoyant or colder columns at -1°C , some of which were initiated in the upper troposphere, were seen nearly side by side with the positive columns. They were clearly indicative of cold moist downdrafts driven by the sublimative and evaporative cooling of hydrometeors. A few colder spots just appeared at the leading edge of the outflow in the PBL. Note that some midlevel air masses still remained buoyant as they moved away from the leading rainband. This is consistent with the above-mentioned rearward-decaying convective cells.

Figure 2c shows the 3-D distribution of vortical tubes with opposite signs, which closely resembles that of buoyant columns. Of interest is the fact that positive and negative midlevel vortical tubes, or VHTs, often appeared in pairs. Based on the given hodograph in the inset of Fig. 2c, they were obviously caused by the tilting of the horizontal vorticity associated with vertical shear, by both updrafts and downdrafts. These significant tilting effects suggest that many updrafts and downdrafts did not collocate with the paired vortices, but instead occurred between them. This differs from VHTs that occur during tropical cyclogenesis in barotropic environments, as discussed by Hendricks et al. (2004). In contrast, the stretching of the absolute vorticity appeared to account for the generation of the lower-level robust cyclonic vortical tubes in the vicinity of the leading convergence zone. It is apparent from Fig. 2c that the VHTs decreased rapidly in both depth and magnitude rearward due to the presence of vertical shear and horizontal deformation, as well as the

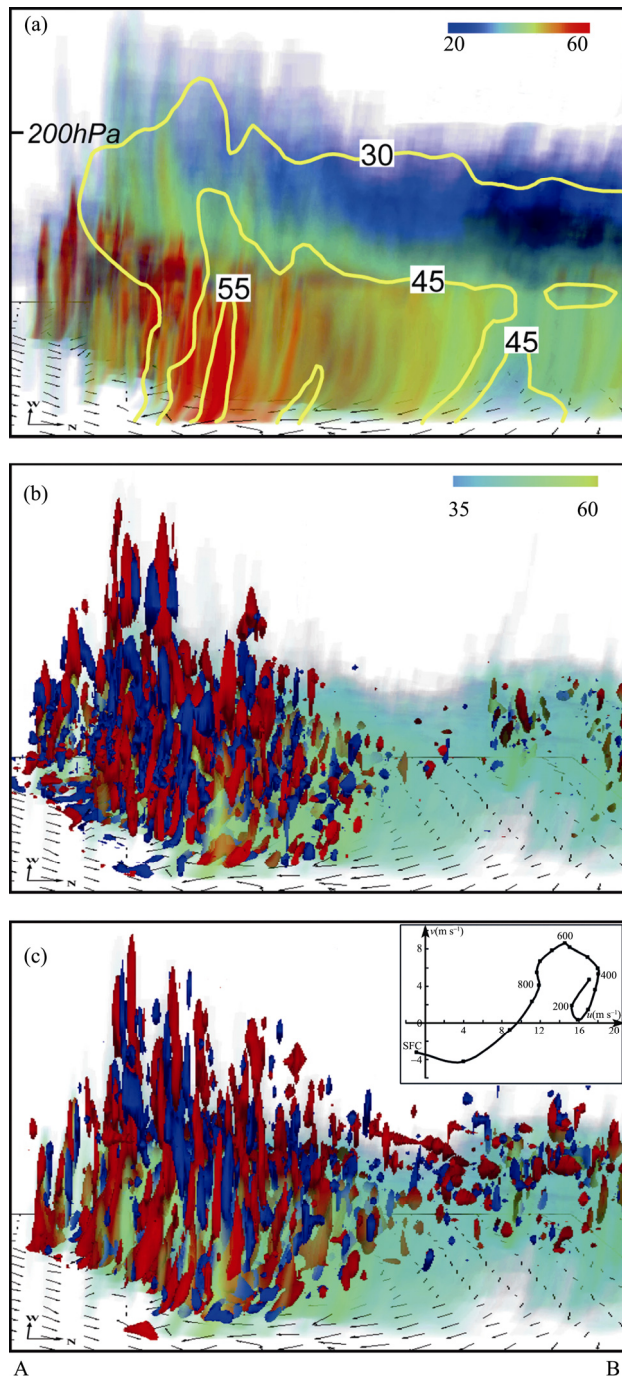


Figure 2 Vis5D plots of (a) radar reflectivity (superposed with its vertical cross section); (b) local buoyancy; and (c) relative vorticity along line AB in Fig. 1c facing west, from the 8-h (D03 and D04) integration valid at 2000 UTC 4 July 2003. In (b) and (c), the red and blue shadings are for isosurfaces of $\pm 1^\circ\text{C}$, $\pm 6 \times 10^{-3} \text{ s}^{-1}$, respectively, whereas the light green shadings indicate volumes of cloudy air. The inset in (c) shows a mean hodograph that is averaged over the MCS area of $150 \text{ km} \times 100 \text{ km}$. Surface winds are plotted every 7.4 km.

mixing of positive and negative vortical tubes. Only weak and short vortical tubes appeared at the midlevel in the trailing stratiform region, where a mesoscale convective vortex (MCV, Zhang and Fritsch, 1987; Zhang, 1992) was located (not shown). Since the trailing precipitating towers could be traced back to their convective origins, the VHTs developed along the leading rainband must have

made some contribution to the development of the MCV in the trailing stratiform region. This will be the subject of a forthcoming article.

4 Summary and concluding remarks

In this study, we have shown the encouraging results of a cloud-resolving model that was used to reproduce a mei-yu frontal MCS and its associated heavy rainfall, as verified against available observations. The use of the finest horizontal resolution of 444 m and the incorporation of a few additional soundings allowed us to produce the more realistic simulation to date, especially compared to those models using convective parameterizations which often overpredict rainfall distribution and underpredict rainfall amounts. Although it is recognized that a single case study cannot provide a rigorous test of the predictability of a cloud-resolving model, the results do indicate that it may be possible to improve summertime quantitative precipitation forecasts associated with the mei-yu fronts, or other midlatitude MCSs, if higher resolution observations and models that utilize more realistic cloud microphysics are used.

It is shown here that, with the Vis5D, the torrential rainfall that produced MCSs consisted of convective hot towers along the leading rainband. These weakened as they were advected rearward, leading to meso- γ -scale inhomogeneity in rain showers in the trailing stratiform region. The associated updrafts and downdrafts generated meso- γ -scale vortical tubes of opposite signs and intense cyclonic vortices in the leading converging zone, which appeared to contribute to the development of an MCV in the stratiform region. The multi-scale interaction between the VHTs, the MCV, and the mei-yu frontal circulations will be examined in a forthcoming journal article.

Acknowledgements. We wish to thank Prof. Y. Ni for providing the field observations used for the present study. This work was supported by Jiangsu Education Science Foundation (Grant No. 07KJB170065), Chinese National Science Foundation (Grant No. 40775060), and U.S. National Science Foundation (Grant No. ATM0758609).

References

- Biggerstaff, M. I., and R. A. Houze Jr., 1991: Kinematic and precipitation structure of the 10–11 June 1985 squall line, *Mon. Wea. Rev.*, **119**, 3034–3065.
- Browning, K. A., J. C. Fankhauser, J.-P. Chalon, et al., 1976: Structure of an evolving hailstorm, Part V: Synthesis and implications for hail growth and hail suppression, *Mon. Wea. Rev.*, **104**, 603–610.
- Chen, S.-J., Y.-H. Kuo, W. Wang, et al., 1998: A modeling case study of heavy rainstorms along the mei-yu front, *Mon. Wea. Rev.*, **126**, 2330–2351.
- Dudhia, J., 1993: A nonhydrostatic version of the Penn State—NCAR mesoscale model: Validation tests and simulation of an Atlantic cyclone and cold front, *Mon. Wea. Rev.*, **121**, 1493–1513.
- Hendricks, E. A., M. T. Montgomery, and C. A. Davis, 2004: The role of “vortical” hot towers in the formation of tropical cyclone Diana (1984), *J. Atmos. Sci.*, **61**, 1209–1232.
- Houze Jr., R. A., 2004: Mesoscale convective systems, *Rev. Geophys.*, **42**, RG4003, doi:10.1029/2004RG000150.
- Kain, J. S., 2004: The Kain-Fritsch convective parameterization: An

- update, *J. Appl. Meteor.*, **43**, 170–181.
- Kato, T., 2006: Structure of the band-shaped precipitation system inducing the heavy rainfall observed over northern Kyushu, Japan on 29 June 1999, *J. Meteor. Soc. Japan*, **84**, 129–153.
- Liu, Y., D.-L. Zhang, and M. K. Yau, 1997: A multiscale numerical study of Hurricane Andrew (1992). Part I: Explicit simulation and verification, *Mon. Wea. Rev.*, **125**, 3073–3093.
- Tao, W.-K., and J. Simpson, 1993: The Goddard cumulus ensemble model. Part I: Model description, *Terr. Atmos. Oceanic Sci.*, **4**, 35–72.
- Zhang, D., and R. A. Anthes, 1982: A high-resolution model of the planetary boundary layer—Sensitivity tests and comparisons with SESAME-79 data, *J. Appl. Meteor.*, **21**, 1594–1609.
- Zhang, D.-L., and J. M. Fritsch, 1987: Numerical simulation of the meso-beta-scale structure and evolution of the 1977 Johnstown flood. Part II: Inertially stable warm-core vortex and the mesoscale convective complex, *J. Atmos. Sci.*, **44**, 2593–2612.
- Zhang, D.-L., 1992: The formation of a cooling-induced mesovortex in the trailing stratiform region of a midlatitude squall line, *Mon. Wea. Rev.*, **120**, 2763–2785.